Environment Economic Power Dispatch from Power System Based on Multi-objective Novel Tree Seed Optimization Algorithm

Gonggui Chen, *Member, IAENG*, Handu Zhuo, Xiaorui Hu, Fangjia Long and Hongyu Long*

***Abstract*—Tree seed algorithm (TSA) is a heuristic search algorithm that deals with low-dimensional issues. To overcome the deficiency of TSA in solving environmental economic power dispatch (EED) problem with high-dimensional, nonlinear, and non-convex characteristics, this article proposes a novel multi-objective tree seed algorithm (MONTSA), which possesses superior ability to obtain Pareto optimal solution (POS) sets. For expanding the search space as well as balancing the ability of exploration and exploitation about TSA, three modification strategies, including dynamic search tendency (*ST*), Gaussian mutation mechanism and variation mechanism of differential evolution algorithm based on Cauchy mutation strategy are adopted to constitute MONTSA. In addition, a constraint handling technique to make sure zero constraint violation and non-inferior sorting approach based on dynamic crowding distance are also put forward. The above introduced strategies allow MONTSA to obtain POS with better distribution. Eight cases, containing four objectives of fuel cost, pollution emission, power loss and fuel cost with valve point effect, are experimented on IEEE 30 bus, IEEE 57 bus and IEEE 118 bus test systems. The results reveal that, compared with MOTSA and MOPSO/MODE, MONTSA is effectively capable of addressing EED problem, which is able to obtain uniformly distributed Pareto frontiers (PFs) and better best compromise solution (BCS). Eventually, the performance indicators *GD* and *HV* show that PFs and BCS obtained by MONTSA are more outstanding than the rest of algorithms, with uniform distribution, strong convergence and powerful stability.**

***Index Terms*—Environment economic power dispatch, novel multi-objective tree seed algorithm, a novel constraint handling technique.**

Manuscript received August 12, 2021; revised November 6, 2021. This work was supported by the National Natural Science Foundation of China under Grant 51207064.

Gonggui Chen is a professor of Key Laboratory of Industrial Internet of Things and Networked Control, Ministry of Education, Chongqing University of Posts and Telecommunications, Chongqing 400065, China; Chongqing Key Laboratory of Complex Systems and Bionic Control, Chongqing University of Posts and Telecommunications, Chongqing 400065, China (e-mail: chenggpower@126.com).

Handu Zhuo is a master degree candidate of Chongqing University of Posts and Telecommunications, Chongqing 400065, China (e-mail: 1404542618@qq.com).

Xiaorui Hu is a professor level senior engineer of Marketing Service Center, State Grid Chongqing Electric Power Company, Chongqing 401123, China (e-mail: xiaorui4832@sina.com).

Fangjia Long is a senior engineer of State Grid Chongqing Electric Power Company, Chongqing 400015, China (e-mail: 157990759@qq.com).

Hongyu Long is a professor level senior engineer of Chongqing Key Laboratory of Complex Systems and Bionic Control, Chongqing University of Posts and Telecommunications, Chongqing 400065, China (corresponding author to provide phone: +8613996108500; e-mail: longhongyu20@163.com).

I. INTRODUCTION

IN modern society, electricity is closely related to life, ranging from family routine to top field. The quality of electricity directly affects whether electricity can be utilized validly. Therefore, it is of great necessity to study how to better electricity quality [1-3].

In the power system, dispatch aims to ensure safe, continuous and stable operation. The early optimization dispatch mainly adopts the economic dispatch (ED). Traditional ED occupies a prominent position. With the rapid economic development, the load demand of power system increases substantially and ED can no longer match the social development. Whereupon the economic load dispatch (ELD) considering load demand is presented. ELD intends to allocate the generation capacity of each unit in an optimal way in the power system, which possesses multiple thermal generators to minimize the fuel cost within the system constraints. It is regarded as the only criterion for evaluating economic benefits [4-7].

Currently, thermal power generation plays a vital role in economic and social development, resulting in the production of harmful gases and carbon dioxide. The harmful gases are mainly nitrogen oxides and sulfur oxides, which not only pollute the environment but also trigger the greenhouse effect. With the deterioration of global ecological environment, governments are also promoting the concept of low-carbon emission reduction and formulating a series of laws and regulations to limit the emission of pollutants. To achieve sustainable development of society, environmental protection factors should be incorporated into ELD that focuses on economic benefits. As a result, EED that takes into account environmental factors and economic benefit factors has emerged [8-10]. EED is a non-linear, high-dimensional and non-convex multi-objective optimization problem (MOP), which possesses a great amount of equality constraints and inequality constraints [11, 12]. In most instances, multiple objectives about EED problem are in a competitive relationship. The key to addressing this problem is choosing appropriate methods to prevent multiple objectives from degrading and provide a better dispatching scheme.

Different from single objective optimization problem, multi-objective optimization problem involves competing objectives and conflicting solutions, where the increase of one objective function will inevitably lead to the decrease of another function. In recent years, it has been a hot topic in solving EED problem. Innumerable scholars primarily concentrate on how to solve the multi-objective function. Normally, a series of POS are found, where the decision maker selects the BCS as a satisfactory solution to EED problem [13, 14]. Due to the non-convexity of EED problem, it is quite difficult to obtain BCS of POS. The principal methods used in the early stage are linear programming method, gradient method and penalty function method [15-17]. On one hand, these methods require multiple runs to obtain solution of problem and cannot obtain the global optimal solution, which consume a great amount of running time; on the other hand, EED problem is multi-peak and non-convex, which leads to that traditional methods are not applicable to EED problem.

The disadvantages of research methods in the early stage lead to single application scenarios and have difficulty in solving EED problem. In view of the drawbacks for these methods, a large number of experts raise to use heuristic search algorithm to solve EED problem. The advantage of heuristic search algorithm is that it can obtain a series of POS in one run without considering the initial state and objective competition. Since this approach was brought forward, a great amount of heuristic search algorithms have been successfully applied to solve EED problem [18-21]. The representative algorithms are multi-objective differential evolution algorithm (MODE) and improved MODE, multi-objective particle swarm algorithm (MOPSO) and enhanced MOPSO, multi-objective moth optimization algorithm (MOMO) and integrated MOMO, non-dominant sorting genetic algorithm (NSGA) and NSGA-II, genetic algorithm (GA) and hybrid search algorithm (HSA), etc. Since TSA was put forward by Kiran in 2015, it has been widely employed in various optimization problems [22]. In literature [23], TSA is used to verify and compare the optimal power flow problem of large power systems. In literature [24], TSA based on integrated search strategy is utilized to solve high-dimensional continuous optimization problem. In literature [25], a sinusoidal tree species algorithm (STSA) is proposed to solve complex high-dimensional optimization problem. In literature [26], TSA is applied to train feed-forward multi-layer perceptron artificial neural network. In literature [27], researchers propose an improved tree species algorithm (ITSA) that takes advantage of Deb sorting rules for constrained optimization. In literature [28], a hybrid chaotic atom search algorithm based on TSA and Levy flight strategy is put forward to solve the optimization problem.

While TSA is applied to MOP, a novel heuristic algorithm Multi-Objective Tree Species Algorithm (MOTSA) is also advanced. The MOTSA has the advantages of simple search stage, few variable parameters and excellent robustness. Nevertheless, the standard MOTSA addressing the EED problem has the following troubles: falling into the local optimal, early or slow convergence and not balancing the capacity of global search and the local search. Therefore, four enhancements are adopted to strengthen the performance of MOTSA. Firstly, the control parameter is transformed into dynamic *ST*. If the *ST* is too large, it will affect the global search. If the *ST* is too small, it will affect the local search. Dynamic *ST* helps balance the global search and the local search. Secondly, the Gaussian mutation mechanism is added. In the local search stage, the Gaussian mutation mechanism produces small-scale disturbances and has desirable local search capability, which is beneficial to avoid falling into the local optimum or premature convergence. Thirdly, DE algorithm variation process based on Cauchy mutation strategy is introduced. In the global search stage, the Cauchy mutation operator can produce larger mutation perturbation and has good global search capability. In combination with DE algorithm, it is favorable to upgrade the convergence ability about TSA. Last one, a constraint handling techniques and non-inferior sorting method based on dynamic crowding distance are posed to maintain the population diversity as well as enhance the extensiveness and uniformity of POS distribution. The above enhancement strategies are integrated with the standard MOTSA to constitute a MONTSA. The several algorithms-MONTSA, MOTSA and MOPSO/MODE are tested in the standard IEEE30 bus, IEEE 57 bus and IEEE 118 bus test systems under the condition that the constraints are not violated in order to verify the MONTSA performance. Furthermore, the *GD* and *HV* metrics are selected to evaluate stability, convergence, and diversity about POS obtained by several algorithms [29-31].

The line structure about this article is as follows: Section II focuses on the mathematical model of EED problem. Section III mainly introduces the original MOTSA and gives the relevant improvement steps. Section IV displays simulation results, performance analysis and evaluation indicators of several algorithms. Section V presents the final conclusion.

II. Mathematical Model

The EED problem refers to the dispatch scheme that minimizes both fuel cost and pollution emissions objectives while satisfying a series of equality constraints and inequality constraints. Due to the requirement of ED, line power loss is also considered as one of research objectives. Hence, the EED problem is essentially a MOP, whose mathematical model is expressed as follows:

$$\text{minimize } F = (f_1(G_P), f_2(G_P), \cdots f_n(G_P)) \tag{1}$$

$$\begin{aligned} H_j\left(G_P\right) \geq 0, j = 1,2,3,\cdots p \\ I_k\left(G_P\right) = 0, k = 1,2,3,\cdots q \end{aligned} \tag{2}$$

where $f_n(G_P)$ represents the *n*th objective function; n represents the number of objective functions; G_P represents the active power output of generator unit; p, q represents the number of inequality constraints and equality constraints, respectively.

The fundamental objective optimization in EED problem is zero violation constraints. The mathematical model about EED problem is principally divided into two categories: objective functions and constraint conditions. The objective functions contain fuel cost, fuel cost with valve point effect, pollutant emissions and network power loss, and the constraint conditions include equality constraints and inequality constraints.

A. Objective Functions

1) Minimization fuel cost

The operation cost in power system chiefly involves variable cost and fixed cost. Variable cost is primarily fuel cost from each unit. Normally, the quadratic function of active power output from each unit is used to express fuel cost (F_{cost}).

$$F_{cost}=\sum_{i=1}^{N_G}(a_i+b_iG_{Pi}+c_iG_{Pi}^2)(\$/\text{h}) \tag{3}$$

where a_i, b_i and c_i represent the fuel coefficients of ith generator unit; G_{Pi} denotes the active power output of ith generator unit; N_G indicates the number of generator unit. The unit of F_{cost} is USD/hour.

As the inlet valve of steam turbine turns off suddenly, it will cause an impulse response superimposed on the unit consumption curve, called valve point effect, which is mathematically described by adding a sinusoidal function on the basis of the quadratic function. From the mathematical model, fuel cost considering valve point effect (F_{cost_vp}) is a non-linear and discontinuous problem and the solution process is particularly complicated.

$$F_{cost\_vp}=\sum_{i=1}^{N_G}(a_i+b_iG_{Pi}+c_iG_{Pi}^2+\left|d_i\times\sin(e_i\times(G_{Pi}^{\min}-G_{Pi}))\right|)(\$/\text{h}) \tag{4}$$

where d_i and e_i are the fuel coefficients with valve point effect; $G_{Pi}^{\min}$ represents the minimum active power output of the ith generator unit. The unit of $F_{cost\text{-}vp}$ is USD/hour.

2) Minimization pollution emissions

The pollution emissions from fossil fuel combustion are generally CO_2, NO_x and SO_x, which are integrated as one model. Thence, the model about generator unit active power output is described as pollution emissions ($E_{mission}$).

$$E_{mission}=\sum_{i=1}^{N_G}\alpha_i+\beta_iG_{Pi}+\gamma_iG_{Pi}^2+\zeta_i\exp(\lambda_iG_{Pi})(\text{t/h}) \tag{5}$$

where α_i, β_i, γ_i, ζ_i and λ_i are the emission coefficients of the ith generator unit. The pollution emissions unit is ton/hour.

3) Minimization power loss

There exists line transmission power loss (P_{loss}) in system structure, which will inevitably have a remarkable influence on safe operation and economic dispatch. Therefore, it is indispensable to regard the power loss as optimization objective. The specific mathematical model is as follows:

$$P_{loss}=\sum_{i}^{N_B}\sum_{j\neq i}^{N_B}g_{ij}\left[V_i^2+V_j^2-2V_iV_j\cos\delta_{ij}\right](\text{MW}) \tag{6}$$

where N_B represents the total number of buses; i and j represent the number of buses; g_{ij} is the conductance of branches between i and j; V_i and V_j are the voltage of buses i and j, respectively; δ_{ij} is the voltage phase angle difference between i and j. The unit of P_{loss} is MW.

B. Constraint conditions

1) Equality constraints

The active power output about generator unit requires to meet two components: load demand and network loss. The general mathematical expression is as follows:

$$\sum_{i=1}^{N_G}G_{Pi}-P_L-P_{loss}=0 \tag{7}$$

The concrete active power and reactive power equations are constrained as follows:

$$\begin{aligned}&G_{Pi}-P_{Li}-V_i\sum_{j=1}^{N_B}V_j(G_{ij}\cos\delta_{ij}+B_{ij}\sin\delta_{ij})=0 \qquad i\in N_G\\&G_{Qi}-Q_{Li}-V_i\sum_{j=1}^{N_B}V_j(G_{ij}\sin\delta_{ij}-B_{ij}\cos\delta_{ij})=0 \qquad i\in N_{PQ}\end{aligned} \tag{8}$$

where G_{Pi} and G_{Qi} represent active power and reactive power injected at bus i, respectively; P_{Li} and Q_{Li} represent active load and reactive load from bus i, respectively; G_{ij} and B_{ij} denote conductance and susceptance between i and j, respectively; N_{PQ} represents the number of load buses.

2) Inequality constraints

To guarantee the safety and economy in power system, inequality constraints should be satisfied, primarily generator unit active output constraints and reactive power output constraints, bus voltage constraints as well as line power flow constraints.

The lower and upper limits about generator unit active power output are restricted as follows:

$$G_{Pi}^{\min}\leq G_{Pi}\leq G_{Pi}^{\max} \tag{9}$$

The limit interval about generator unit reactive power output is constrained as follows:

$$G_{Qi}^{\min}\leq G_i\leq G_{Qi}^{\max} \tag{10}$$

The extreme range about bus voltage constraints is as follows:

$$V_i^{\min}\leq V_i\leq V_i^{\max} \tag{11}$$

Arbitrary lines own its maximum transmission capacity. To assure the stable operation in power system, line flow constraints are designed as follows:

$$p_{lf,m}\,|\leq p_{lf,m}^{\max} \qquad m\in l \tag{12}$$

where $p_{lf,m}$ represents the active power of the mth line, $p_{lf,m}^{max}$ indicates the maximum active power that the mth line can withstand, l is the number of transmission lines.

III. RESEARCH ON TSA FOR EED PROBLEM

A. Synopsis of MOTSA

MOTSA is a meta-heuristic algorithm based on the relationship between trees and their seeds in nature, which is mainly applied to the field about population-based search. Similar to other heuristics, MOTSA is an iterative search algorithm based on population with randomized solutions. The location of trees and their seeds in the search space correspond to the solution of optimization problem. The tree produces more than a seed and the better seed position is replaced by the tree position. While a new position about tree seed is generated, the global optimal position or another tree position is taken as the tree position. During each iteration, MOTSA employs two search equations to update seed positions, namely the global search equation and the local search equation, which solve the optimization problem in terms of both exploration and exploitation. Furthermore, the two search phases can be switched by adjusting ST.

1) Global search phase (ST > 0.5)

In the global search phase, to ensure extensive exploration, the search equation is designed based on the spread-out population principle. For EED optimization problem, tree population individuals are searched from multiple points in the search space and randomly interact in the population. The iterative search in the global phase selects two different trees to generate new seeds, whose search equation is as follows:

$$X_i(t+1)=X_i(t)+r*\left(X_i(t)-X_{rand}(t)\right) \tag{13}$$

where $X_i(t+1)$ is the seed position produced by the current ith tree, $X_i(t)$ is the current ith tree position, $X_{rand}(t)$ is the random tree position selected in the population, the random number *rand* is different from *i*, *r* is the step factor, which is a random number in the range [-1,1] and mathematical expression is as follows:

$$r = -1 + 2 * r_1 \tag{14}$$

where r_1 is a random number in the range [0,1].

2) Local search phase (ST < 0.5)

In the local search phase, a seed mechanism is dished to compensate overutilization. The number of seeds generated by a tree is random and the location of generated seeds is vital to optimization problem, which constitute the core of local search. The iterative search in the local phase uses the location of random tree and the current optimal individual location of tree population. The search equation is described as follows:

$$X_i(t+1) = X_i(t) + r * \left(X_{best}(t) - X_{rand}(t)\right) \tag{15}$$

where $X_{best}(t)$ is the best individual in the population.

B. MONTSA

1) Dynamic search tendency

In the MOTSA, the size of *ST* has an impact on the balance between the global search and the local search. Additionally, *ST* plays an important role in the algorithm solution and fast convergence. For one thing, if the upper limit is too large, the global search phase will be executed, which leads to slow convergence and cannot obtain an accurate global optimal solution. For another, if the lower limit is too small, the ability to implement local search is stronger and it is easy to fall into local optimal as well as fast convergence, which is unable to converge to optimal solution. In accordance with the change of iteration numbers, an adaptive nonlinear *ST* is put forward. The former is so large that search process tends to the global search, which has the advantage of avoiding the local optimum. The latter is exceedingly inclined to local search, which is conducive to convergence to optimum solution. The dynamic *ST* is defined as follows:

$$ST = 0.1 + 0.7 * \mathrm{e}^{-5*\sin(\frac{\pi t}{2t_{\max}})} \tag{16}$$

where t is the current number of iterations; $t_{\max}$ is the maximum number of iterations.

2) Gaussian mutation mechanism

In the local search phase of MOTSA, the population optimal individual is barely utilized in a simple way and information hidden is not utilized fully. Similar to other intelligent algorithms, MOTSA is prone to falling into local optimum or convergence ahead of time, resulting in that algorithm performance gets deteriorated [32]. Inspired by the update mechanism of improved PSO, the Gaussian mutation mechanism is introduced into the tree seeds search process, which is described as follows in detail:

$$X_{i,j}(t+1) = N\left(\frac{X_{best,j}(t) + X_{rand,j}(t)}{2}, \left|X_{rand,j}(t) - X_{best,j}(t)\right|\right) \tag{17}$$

where $j \in \{1,2,3,...,D\}$ is a dimension randomly selected, which is conducive to maintaining diversity and has the feature of computational simplicity. After introducing the Gaussian mutation operator, the search space position formed by the current solution $X_{rand}(t)$ and the current optimal solution $X_{best}(t)$ generates new candidate solutions, which gradually encompass center position between $X_{rand}(t)$ and $X_{best}(t)$. As the number of iterations increases, population individuals will approach the current optimal solution $X_{best}(t)$. Meanwhile, dynamic search tendancy will turn to another phase -exploitation.

3) DE algorithm variation process based on Cauchy mutation strategy

To ensure extensive exploration and heighten the global search capability of MOTSA, the variation process of DE algorithm is introduced. Inversely, owing to the fact that DE algorithm has less and less population variation in the late iteration, it leads to the deterioration of individual diversity and to a certain extent, it no longer has the ability to explore. Moreover, DE algorithm is extremely sensitive to parameters. If parameters are set unreasonably, it will account for population falling into the local optimum and search will stagnate. For the drawbacks of traditional DE algorithm, a novel DE variation strategy is assimilated. DE algorithm has 6 variational strategies. In line with literature [33], the DE/rand/1 variation strategy has a relatively balanced performance when solving unimodal and multimodal functions, especially solving multimodal functions. The control parameters of traditional DE algorithm are constant. For picking up convergence speed and ameliorate global search ability of the algorithm, the Cauchy mutation strategy is introduced to replace scaling factor [34]. Cauchy mutation strategy can generate large variances, which helps to avoid falling into the local optimum. A novel DE/rand/1 variation strategy is specific as follows:

$$X_i(t+1) = X_{rand1}(t) + Cauchy(0,1) * \left(X_{rand2}(t) - X_{rand3}(t)\right) \tag{18}$$

where $X_{rand1}(t)$, $X_{rand2}(t)$ and $X_{rand3}(t)$ are three arbitrarily chosen different individuals in the population.

4) Constraint handling technique and non-inferior sorting based on dynamic crowding distance

■ *Constraint handling technique*

The inequality constraints in EED problem are divided into control variable inequality constraints and state variable inequality constraints. The constraint conditions of control variable inequality are the active power output of generator, which is supposed to be adjusted according to the following rules (19) when population individuals violate specified range.

$$g_i = \begin{cases} g_{i\min} & if\ g_i < g_{i\min} \\ g_i & if\ g_{i\min} < g_i < g_{i\max} \\ g_{i\max} & if\ g_i > g_{i\max} \end{cases} \tag{19}$$

The constraint conditions of state variable inequality are generator reactive power output, generator bus voltage and line flow. The total violation value that violates state variable inequality constraint is represented by (20) when the specified range is violated by population individuals.

$$Constr(g_p) = \sum_j \max(h_j(g_p, x), 0) \tag{20}$$

where $Constr(g_p)$ denotes total violation value that violates state variable inequality constraint and $h_j(g_p,x)$ manifests the jth violation value that violates state variable inequality constraint.

Randomly select two individuals g_{pm} and g_{pn} from the population as well as calculate and compare total violation constraints values $Constr(g_{pm})$ and $Constr(g_{pn})$. Judge the dominant relationship between two individuals according to following rules.

Constraint Handling Techniques:

if $Constr(g_{pm}) < Constr(g_{pn})$ g_{pm} dominates g_{pn};
if $Constr(g_{pm}) > Constr(g_{pn})$ g_{pm} dominates g_{pn};
if $Constr(g_{pm}) == Constr(g_{pn})$
  if $f_i(g_{pm}) \le f_i(g_{pn})$ $\forall$ $i \in \{1, 2, \ldots, M\}$ and
  $f_j(g_{pm}) < f_j(g_{pn})$ $\exists$ $j \in \{1, 2, \ldots, M\}$
    g_{pm} dominates g_{pn};
  else
    g_{pm} is dominated by g_{pn}.

In accordance with above dominant rules, all individuals in the population are divided into n levels. Each level corresponds to single or multiple individuals and the value corresponding to each level is $rank(i)$. The smaller the $rank(i)$ is, and the higher the individual priority is. As the $rank(i)$ from different individuals are same, the following rules are employed.

■ *Non-inferior sorting based on dynamic crowding distance*

After the population is processed by above constraint handling techniques, there exist different individuals with the same level within the population. The traditional handling techniques is to calculate crowded distance $distance(i)$ according to the non-inferior sorting method proposed by Deb[35], which judges crowded distance of same level individuals and determine priority different individuals. The larger the $distance(i)$ is, the higher priority of individual i is. Paradoxically, the traditional method will result in uneven distribution of PFs and not fully reflecting neighborhood information. In response to this problem, a dynamic crowding distance calculation method is introduced to make POS more uniform and maintain the diversity of population.

Constraint Handling Techniques:

if $rank(x_i) < rank(x_j)$ i dominates j;
if $rank(x_i) > rank(x_j)$ j dominates i;
if $rank(x_i) == rank(x_j)$
  if $distance(x_i) > distance(x_j)$
    i dominates j;
  else
    j dominates i.

Integrating above mechanism strategies into MOTSA, an enhanced MOTSA is constituted. MONTSA overcomes original deficiency being unable to handle high-dimensional optimization problems, whose pseudo code is listed as follows:

Set the population size N and the problem dimension D;
Set the dynamic search trend ST, the maximum number of iterations t_{max};
Select the global optimal individual x_{best};
t=1;
while $t < t_{max}$
  for i=1 to N
    if $rand<ST$
      $x(i)=x(r_1)+Cauchy(0,1)*(x(r_2)-x(r_3))$;
    else
      for j=1 to D
        $x(ij)=N(\mu,\sigma)$;
      end for
    end if
  end for
Judge the dominant relationship between x_{new} and x_{best} according to constraint handling techniques and non-inferior sorting method based on dynamic crowding distance
if x_{new} dominates x_{best}
  $x_{best}=x_{new}$;
else
  The global optimal solution x_{best} remains constant;
end if
Output the current PFs and the current global optimal solution;
t++;
end while

C. Application of MONTSA in EED problem

For testing effectiveness of proposed algorithm, it is applied to the EED problem and obtains a collection of non-dominated solutions from PFs. By means of non-inferior sorting method, BCS can be selected from POS to obtain updated global optimal solution after the iteration is terminated. Fig. 1 provides the flow chart about MONTSA how to solve EED problem.

IV. SIMULATION RESULTS AND COMPARISONS

To examine the practicality of enhanced algorithm applied to test systems, not only six bi-objective optimization cases are experimented, but also MOPSO/MODE and MOTSA are selected as comparative algorithms. The several algorithm optimization cases are distributed in IEEE 30, IEEE 57, IEEE 118 bus standard systems in MATLAB 2016b and a PC with Intel(R) Core(TM) i5-7400CPU@3.3GHz with 8GB RAM. Four optimization objectives are: fuel cost, fuel cost with valve point effect, pollution emissions and power loss.

A. Parameter configurations

For the high dimension of EED problem and the complexity of network structure, it is vital to set the appropriate population size and iteration number. The Pareto curves obtained vary for different iteration times. Having repeated experiments, the parameter settings for several algorithms are illuminated in literature [1, 18].

The IEEE 30 bus system is a general test system with a relatively simple and representative structure, including six generator units and a series of other compensation devices. The fuel coefficients and emission coefficients are illustrated in TABLE I, the line data and bus data are in literature [36] and the detailed data is in literature [37]. The structure of IEEE 30 bus system is represented in Fig. 2.

The IEEE 57 bus system is a medium system. Compared with IEEE 30 bus standard system, structure is slightly more complicated. The fuel coefficient and emission coefficient are in literature [2] and the detailed data of system structure is in literature [37]. The structure of IEEE 57 bus system is indicated in Fig. 3.The IEEE 118 bus system is a complex system, whose data is presented in literature [31]. The structure of IEEE 118 bus system is expressed in Fig. 4.

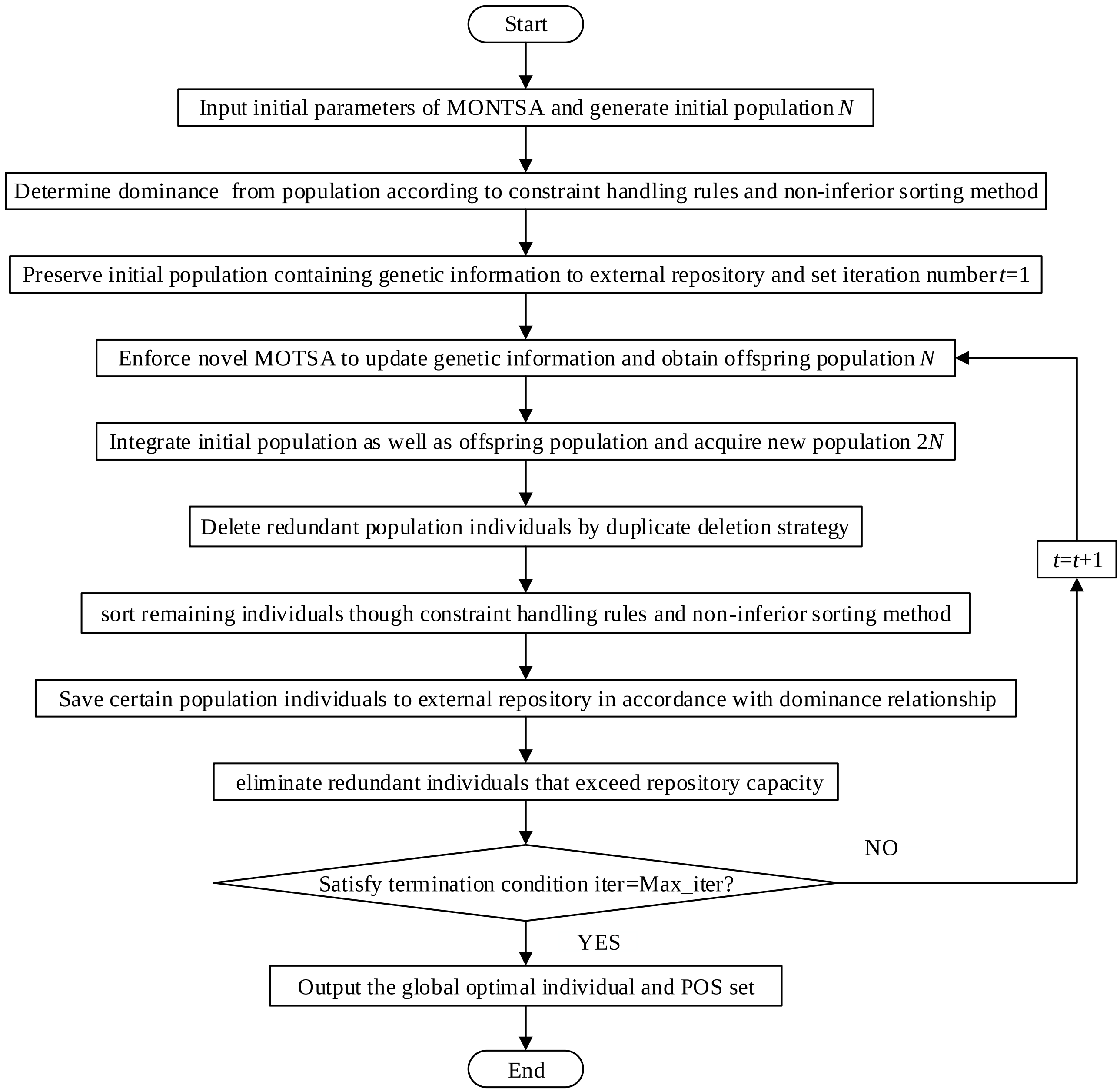

Fig. 1.The flow chart of MONTSA to solve EED problem

B. IEEE 30 test system

1) Case 1: Optimization experiment about F_{cost} and $E_{mission}$

To effectively solve practical problem, MOP requires finding BCS from multiple objectives simultaneously. In Case 1, the PFs obtained by MONTSA, MOTSA and MOPSO are shown in Fig. 5, whose distinction is considerably apparent. Meanwhile, it can be seen that compared with MOTSA and MOPSO, PF obtained by MONTSA is particularly uniform and is superior to the rest of comparative algorithms. Fig. 6 grants extreme solutions both fuel cost and pollution emissions. Besides, it reveals BCS obtained by MONTSA.

TABLE II denotes BCS obtained by three algorithms and corresponding generator units active power output. Furthermore, it also enumerates comparison results from literature to uphold the proposed algorithm. In TABLE II, BCS for MONTSA is 0.1972 (t/h) and 621.09 ($/h), which dominates BCS for the rest of algorithms. TABLE III and TABLE IV give the lower emission and fuel cost from three algorithms and published literature. The lower emission and fuel cost obtained by improved algorithm are 0.1942 (t/h) and 611.10 ($/h), respectively. It indicates that MONTSA can obtain better extreme solutions.

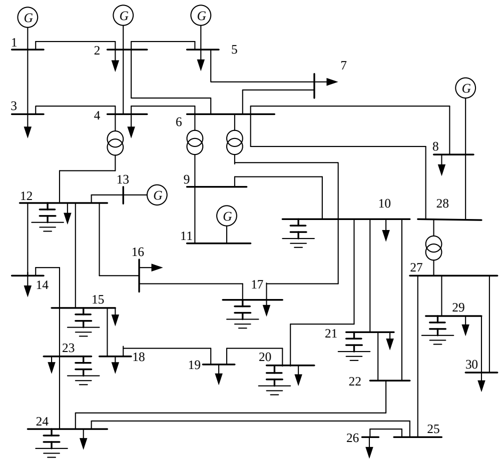

Fig. 2. The network structure of IEEE 30

2) Case 2: Optimization experiment about $F_{cost\text{-}vp}$ and $E_{mission}$

The valve point effect from generator unit results in a non-convex and non-differentiable fuel cost curve. Thence, it is necessary to utilize the relevant intelligent algorithm to solve EED problem. Considering the valve point effect, Case 2 aims at obtaining the optimal solution of fuel cost with valve point effect and pollution emissions simultaneously. Fig. 7 indicates the PFs obtained by three algorithms, where MONTSA acquires a PF with extreme uniform distribution, and it can be apparently seen that MONTSA has a positive impact on responding relevant problem. Fig. 8 lists the lower pollutant emissions and fuel cost with valve point effect. Moreover, it enumerates BCS obtained by MONTSA.

The BCS for Case 2 obtained by three algorithms and the active output of generator units corresponding to BCS are given in TABLE V. Meanwhile, it cites the data results from the comparison literature. The BCS obtained by MONTSA is 0.1965 (t/h) and 637.32 ($/h), which is superior to comparison algorithms and published literatures. The lower emission and fuel cost with valve point effect obtained by three algorithms and comparative literatures are supplied in TABLE VI, where the extreme emission and fuel cost obtained by proposed algorithm are 0.1942 (t/h) and 625.07 ($/h).To some extent, it concludes that MONTSA has a certain superiority.

3) Case 3: Optimization experiment about P_{loss} and $E_{mission}$

Owing to the fact that power balance is indispensable in line structure, it is obvious that power loss will have a conspicuous influence on economic operation from power system. To assure practical system stable operation in EED problem, the power loss is also considered as an optimization objective. Fig. 9 lists PFs obtained by three algorithms, where MONTSA has better convergence. Fig. 10 represents the lower emission, power loss and BCS obtained by MONTSA.

TABLE VII means BCS of Case 3 obtained by three algorithms as well as corresponding generator units active power output. In addition, TABLE VII also gives specific data results from comparative literature. The BCS obtained by MONTSA surpasses the comparative algorithms and the published literatures, which is 0.1998 (t/h) and 1.3872 (MW). TABLE VIII enumerates the lower emission and power loss obtained by three algorithms and relevant literatures, where the lower emission and power loss obtained by integrated algorithm are 0.1942 (t/h) and 1.0875 (MW). It clearly indicates that MONTSA has a strong ability to obtain a satisfactory optimal solution and extreme solution.

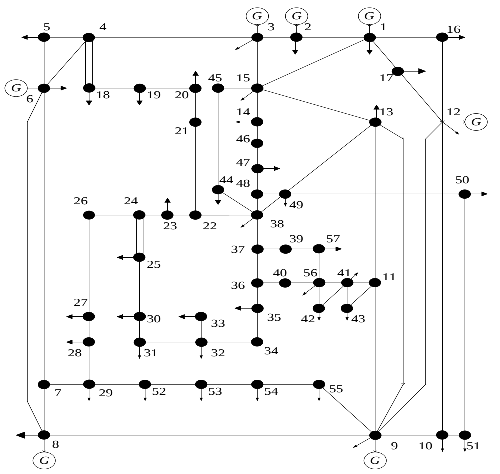

Fig. 3.The network structure of IEEE 57

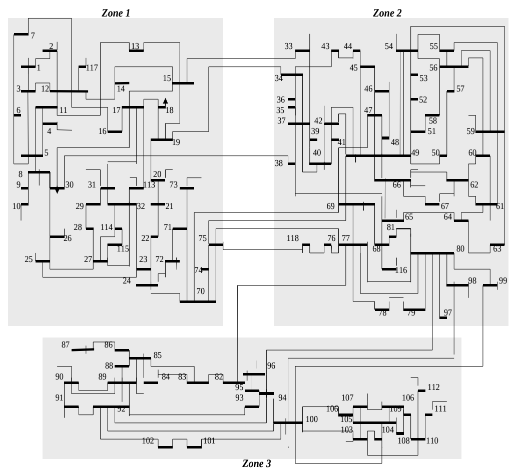

Fig. 4.The network structure of IEEE 118

TABLE I

FUEL AND EMISSION COEFFICIENTS FOR GENERATOR IN IEEE 30 STANDARD SYSTEM

Generators	a	b	c	$G_P^{\min}$	$G_P^{\max}$	α	β	γ	ζ	λ
G_1	10	200	100	5	150	0.04091	-0.05554	0.06490	0.0002	2.857
G_2	10	150	120	5	150	0.02543	-0.06047	0.05638	0.0005	3.333
G_5	20	180	40	5	150	0.04258	-0.05094	0.04586	0.000001	8.000
G_8	10	100	60	5	150	0.05326	-0.03550	0.03380	0.002	2.000
G_{11}	20	180	40	5	150	0.04258	-0.05094	0.04586	0.000001	8.000
G_{13}	10	150	100	5	150	0.06131	-0.05555	0.05151	0.00001	6.667

TABLE II

THE BCS AND CORRESPONDING POWER FOR CASE 1

Generators	MONTSA	MOTSA	MOPSO	MONWOA[1]	SPEA[21]	MBFA[9]	DE[18]	MOPSO[19]	NSGA-II[38]
G_1(MW)	0.3085	0.3087	0.2919	0.3064	0.3052	0.2983	0.3877	0.2882	NA
G_2(MW)	0.4011	0.4012	0.4052	0.4019	0.4389	0.4332	0.5201	0.3965	NA
G_5(MW)	0.5546	0.5671	0.5625	0.5699	0.7163	0.7350	0.2538	0.7320	NA
G_8(MW)	0.5935	0.5972	0.6119	0.5890	0.6978	0.6899	0.7281	0.7520	NA
G_{11}(MW)	0.5472	0.5386	0.5471	0.5419	0.1552	0.1569	0.4655	0.1489	NA
G_{13}(MW)	0.4482	0.4447	0.4454	0.4436	0.5507	0.5503	0.5101	0.5463	NA
F_{cost}($/h)	**621.09**	621.89	622.05	621.12	629.59	629.56	626.03	626.10	625.36
$E_{mission}$(t/h)	**0.1972**	0.1973	0.1978	0.1972	0.2079	0.2080	0.1979	0.2106	0.1984

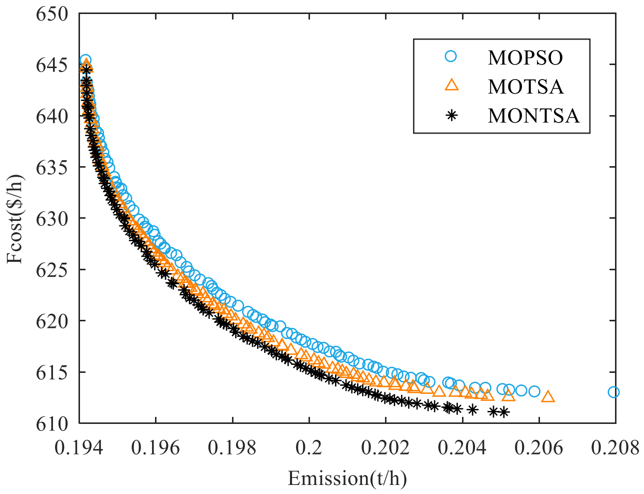

Fig. 5.The PFs obtained by several algorithms in Case 1

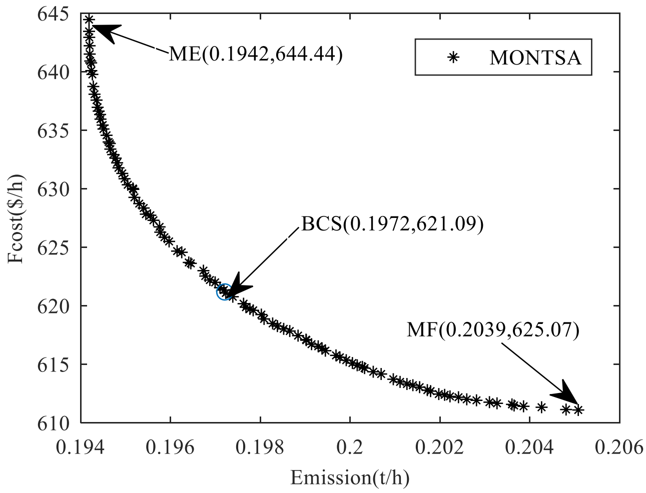

Fig. 6.The PF from MONTSA in Case 1

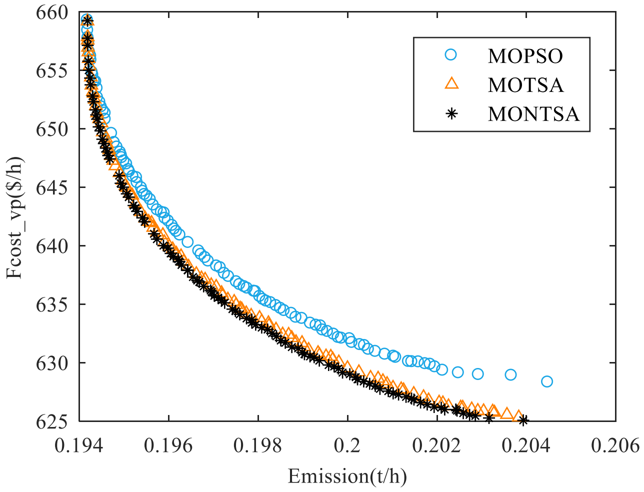

Fig. 7. The PFs obtained by several algorithms in Case 2

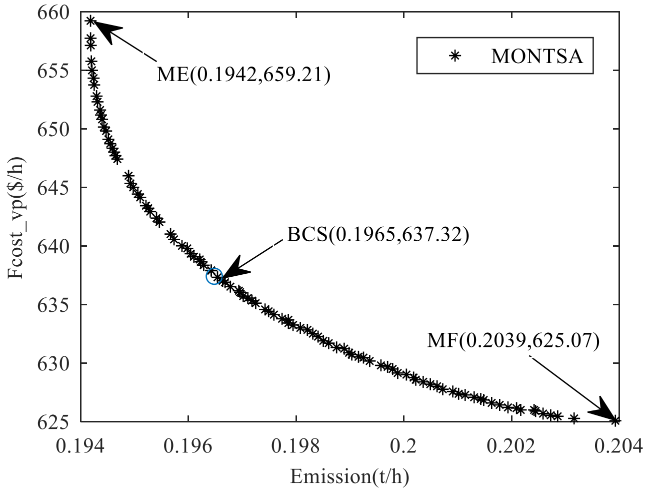

Fig. 8. The PF from MONTSA in Case 2

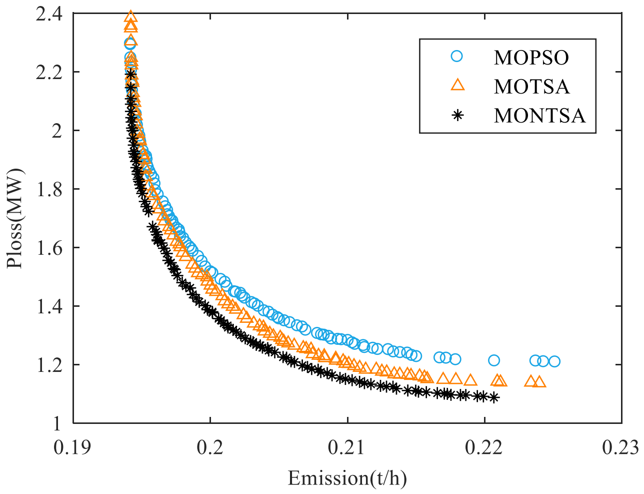

Fig. 9. The PFs obtained by several algorithms in Case 3

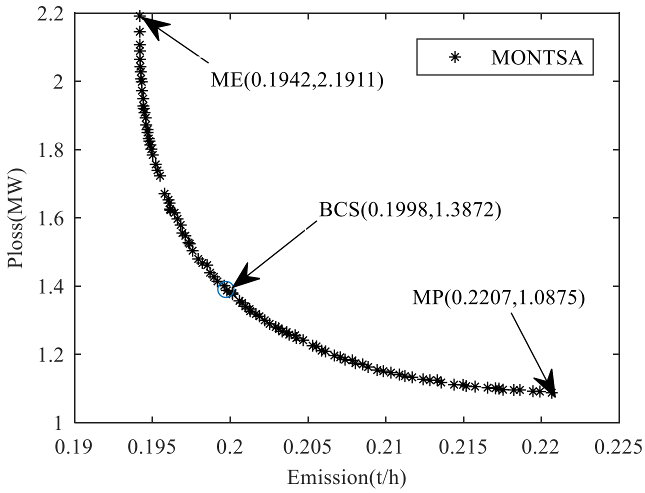

Fig. 10. The PF from MONTSA in Case 3

TABLE III

THE *ME* AND CORRESPONDING POWER FOR CASE 1

Generators	MONTSA	MOTSA	MOPSO	MONWOA[1]	SPEA[21]	MBFA[9]	MOPSO[19]	NSGA[8]	NSBF[39]
G_1(MW)	0.4118	0.4126	0.4056	0.4113	0.3052	0.4716	0.4589	0.4403	0.4047
G_2(MW)	0.4673	0.4647	0.4698	0.4574	0.4389	0.5127	0.5121	0.4940	0.4533
G_5(MW)	0.5413	0.5456	0.5476	0.5398	0.7163	0.6189	0.6524	0.7509	0.5439
G_8(MW)	0.3857	0.3852	0.3936	0.3934	0.6978	0.5032	0.4331	0.5060	0.3921
G_{11}(MW)	0.5403	0.5388	0.5445	0.5411	0.1552	0.1788	0.1981	0.1375	0.5454
G_{13}(MW)	0.5130	0.5143	0.5068	0.5143	0.5507	0.5822	0.6129	0.5364	0.5246
F_{cost}($/h)	644.48	644.87	645.33	643.0	629.59	651.93	656.87	649.24	644.41
$E_{mission}$(t/h)	**0.1942**	0.1942	0.1942	0.1942	0.2079	0.2019	0.2014	0.2048	0.1942

TABLE IV

THE *MF* AND CORRESPONDING POWER FOR CASE 1

Generators	MONTSA	MOTSA	MOPSO	MONWOA[1]	SPEA[21]	MBFA[9]	MOPSO[19]	NSGA[8]	NSBF[39]
G_1(MW)	0.1561	0.1364	0.1331	0.1569	0.1319	0.1175	0.1524	0.1358	0.1780
G_2(MW)	0.3602	0.3366	0.3119	0.3625	0.3654	0.3617	0.3427	0.3151	0.3366
G_5(MW)	0.6475	0.6837	0.7102	0.6220	0.7791	0.7899	0.7857	0.8418	0.7292
G_8(MW)	0.7059	0.6893	0.7144	0.7089	0.9282	0.9591	1.0180	1.0431	0.5908
G_{11}(MW)	0.5821	0.6079	0.5973	0.590	0.1308	0.1457	0.0995	0.0631	0.5766
G_{13}(MW)	0.3987	0.3992	0.3923	0.4114	0.5292	0.4916	0.4669	0.4664	0.4474
F_{cost}($/h)	**611.10**	612.46	612.94	611.23	619.60	618.06	618.54	620.87	619.61
$E_{mission}$(t/h)	0.2051	0.2062	0.2080	0.2048	0.2244	0.2264	0.2308	0.2368	0.2027

TABLE V

THE BCS AND CORRESPONDING POWER FOR CASE 2

Generators	MONTSA	MOTSA	MOPSO	MONWOA[1]	PSO[40]
G_1(MW)	0.3232	0.3217	0.3023	0.3111	0.1409
G_2(MW)	0.4065	0.3972	0.4094	0.4174	0.3442
G_5(MW)	0.5568	0.5578	0.5581	0.550	0.6756
G_8(MW)	0.5700	0.5696	0.5780	0.5718	0.8397
G_{11}(MW)	0.5400	0.5499	0.5488	0.5371	0.4904
G_{13}(MW)	0.4568	0.4591	0.4613	0.4663	0.3980
F_{cost_vp}($/h)	**637.32**	637.58	638.64	638.68	639.65
$E_{mission}$(t/h)	**0.1965**	0.1966	0.1969	0.1966	0.2111

TABLE VI

THE CONCRETE RESULTS ABOUT MF_{VP} AND *ME* FOR CASE 2

Algorithm	Object	Generators						F_{cost_vp}	$E_{mission}$
		G_1	G_2	G_5	G_8	G_{11}	G_{13}		
MONTSA	MF_{vp}	0.1805	0.3550	0.6508	0.7020	0.5396	0.4226	**625.07**	0.2039
	ME	0.4116	0.4631	0.5374	0.3948	0.5413	0.5173	659.21	**0.1942**
MOTSA	MF_{vp}	0.1844	0.3584	0.6270	0.7273	0.5644	0.4118	625.33	0.2038
	ME	0.4125	0.4600	0.5455	0.3937	0.5412	0.5128	659.17	0.1942
MOPSO	MF_{vp}	0.1624	0.3724	0.6235	0.7015	0.6014	0.3960	628.30	0.2045
	ME	0.4084	0.4583	0.5407	0.3959	0.5368	0.5210	659.25	0.1942
MONWOA[1]	MF_{vp}	0.1793	0.3643	0.5970	0.7067	0.5920	0.4136	627.12	0.2038
	ME	0.4108	0.4625	0.5438	0.3903	0.5414	0.5109	659.35	0.1942
PSO[41]	MF_{vp}	0.0994	0.3625	0.4835	0.8736	0.6643	0.3900	626.96	0.2139
	ME	0.3788	0.3932	0.4995	0.5344	0.5734	0.4865	659.44	0.1957

TABLE VII

THE BCS AND CORRESPONDING POWER FOR CASE 3

Generators	MONTSA	MOTSA	MOPSO	MONWOA[1]
G_1(MW)	0.2508	0.2296	0.2401	0.2202
G_2(MW)	0.4060	0.3844	0.3788	0.3821
G_5(MW)	0.7865	0.8026	0.8021	0.8077
G_8(MW)	0.4050	0.4227	0.4371	0.4311
G_{11}(MW)	0.5838	0.5957	0.6029	0.6038
G_{13}(MW)	0.4158	0.4131	0.3876	0.4046
P_{loss}(MW)	**1.3872**	1.4161	1.4652	1.5496
$E_{mission}$(t/h)	**0.1998**	0.2010	0.2012	0.2016

TABLE VIII

THE CONCRETE RESULTS ABOUT *MP* AND *ME* FOR CASE 3

Algorithm	Object	Generators						P_{loss}	$E_{mission}$
		G_1	G_2	G_5	G_8	G_{11}	G_{13}		
MONTSA	*MP*	0.0697	0.2767	1.0203	0.4946	0.6486	0.3349	**1.0875**	0.2207
	ME	0.4135	0.4626	0.5427	0.3868	0.5352	0.5150	2.1911	**0.1942**
MOTSA	*MP*	0.2692	0.3068	1.0606	0.4403	0.6360	0.3747	1.1363	0.2240
	ME	0.4113	0.4583	0.5363	0.3891	0.5456	0.5173	2.3841	0.1942
MOPSO	*MP*	0.1515	0.3464	1.0584	0.4841	0.6318	0.3102	1.2070	0.2252
	ME	0.4065	0.4673	0.5493	0.3970	0.5297	0.5070	2.2935	0.1942
MONWOA[1]	*MP*	0.2200	0.2964	0.8408	0.4853	0.6402	0.3636	1.2423	0.2235
	ME	0.4112	0.4623	0.5452	0.3884	0.5452	0.5079	2.6211	0.1942

C. IEEE 57 test system

1) Case 4: Optimization experiment about F_{cost} and $E_{mission}$

Compared with IEEE 30 bus standard system, IEEE 57 bus test system is slightly more complicated. Fig. 11 states PFs obtained by three algorithms, whose discrimination degree is fuzzy. Consequently, it is of great necessity to locally enlarge BCS of PFs. It is clear that PF obtained by MONTSA has wider distribution. Fig. 12 provides the lower emission, fuel cost and BCS obtained by MONTSA.

The BCS obtained by three algorithms for Case 4 and the active output of generator units corresponding to BCS are granted in TABLE IX. The BCS obtained by MONTSA is better than MOTSA and MOPSO, which is 1.2624 (t/h) and 43117.58 ($/h), respectively. The extreme emission and fuel cost obtained by three algorithms are provided in TABLE X, where the extreme emission and fuel cost obtained by

MONTSA are 1.0327 (t/h) and 41643.66 ($/h), respectively, which precedes MOTSA and MOPSO. It reveals that the proposed algorithm has superior advantages.

2) Case 5: Optimization experiment about P_{loss} and $E_{mission}$

The P_{loss} and $E_{mission}$ optimization has good revenue simultaneously. Fig. 13 signifies PFs obtained by three algorithms, where MONTSA has a smaller distance from PF acquired by MOTSA, whereas a larger distance from PF obtained MOPSO, with better convergence. Fig. 14 gives the lower emission, power loss and BCS obtained by MONTSA.

TABLE XIII reveals BCS obtained by three algorithms as well as corresponding generator unit active power output. The BCS obtained by MONTSA is 1.1241 (t/h) and 12.97 (MW), which is obviously better than results from MOTSA and MOPSO. TABLE XI lists the extreme emission and power loss obtained by three algorithms, where the lower emission and power loss obtained by MONTSA are 1.0319 (t/h) and 8.96 (MW). The extreme result is superior to the rest of algorithms. To an extent, it indicates that MONTSA has an obvious ascendancy.

3) Case 6: Optimization experiment about $F_{cost\text{-}vp}$ and $E_{mission}$

In contrast to IEEE 30 system, the IEEE57 system is similar to the real power system with complex structures. Besides, solving multi-objective complicated optimization problems considering valve point effect poses a challenge to the novel algorithm. Case 6 aims to simultaneously optimize the $F_{cost\text{-}vp}$ and $E_{mission}$ with valve point effect, which will further demonstrate the practicality from MONTSA. The PFs obtained by several algorithms are given in Fig. 15 and it can be clearly seen that the PF obtained by MONTSA is uniformly distributed and consistent through local magnifying. The BCS obtained by MONTSA is listed in Fig. 16. Meanwhile, it provides the upper and lower bounds in the feasible domain.

TABLE XIV not only presents the BCSs obtained by several algorithms, but also shows the corresponding active power output. The BCS is 1.2117t/h and 44673.62$/h, which proves that MONTSA prevails over the classical algorithm. TABLE XII indicates the lower limits about optimization solutions obtained by several algorithms. The lower limit obtained by MONTSA are 1.0363 t/h and 42697.43 $/h, which are distinctly superior to another two algorithms. It turns out that the proposed algorithm is more reliable in addressing optimization issues.

TABLE IX
THE BCS AND CORRESPONDING POWER FOR CASE 4

Generators	MONTSA	MOTSA	MOPSO
G_1(MW)	217.10	219.94	220.87
G_2(MW)	99.84	99.88	100
G_3(MW)	91.69	90.59	89.09
G_6(MW)	99.94	99.84	100
G_8(MW)	338.70	343.88	346.21
G_9(MW)	99.83	99.99	100
G_{12}(MW)	316.85	311.60	310.60
F_{cost}($/h)	**43117.58**	43172.33	43180.3
$E_{mission}$(t/h)	**1.2624**	1.2673	1.2738

TABLE X
THE CONCRETE RESULTS ABOUT *MF* AND *ME* FOR CASE 4

Algorithm	Object	Generators							F_{cost}	$E_{mission}$
		G_1	G_2	G_3	G_6	G_8	G_9	G_{12}		
MONTSA	*MF*	141.90	99.99	41.09	99.84	433.15	99.97	348.21	**41643.66**	1.8143
	ME	327.52	100	140	100	265.11	100	238.15	48329.08	**1.0327**
MOTSA	*MF*	137.95	99.81	43.22	99.79	435.45	99.99	349.68	41710.4	1.8367
	ME	324.15	99.89	140	99.88	264.75	100	243.78	48270.13	1.0382
MOPSO	*MF*	134.57	100	47.02	100	441.36	100	344.19	41751.08	1.8673
	ME	329.46	100	140	100	263.26	100	240.76	48499.83	1.0387

TABLE XI
THE CONCRETE RESULTS ABOUT *MP* AND *ME* FOR CASE 5

Algorithm	Object	Generators							P_{loss}	$E_{mission}$
		G_1	G_2	G_3	G_6	G_8	G_9	G_{12}		
MONTSA	*MP*	122.43	96.80	139.81	99.99	290.73	99.99	410	**8.96**	1.4164
	ME	330.62	99.98	140	99.98	266.70	99.98	233.44	19.90	**1.0319**
MOTSA	*MP*	127.70	90.75	137.19	99.80	294.63	99.99	410	9.25	1.4281
	ME	336.17	100	139.95	100	262.70	100	232.85	20.87	1.0334
MOPSO	*MP*	111.91	100	140	100	299.62	100	410	10.73	1.4363
	ME	332.30	100	140	100	263.80	100	236.71	22.02	1.0365

TABLE XII
THE CONCRETE RESULTS ABOUT MF_{VP} AND *ME* FOR CASE 6

Algorithm	Object	Generators							F_{cost_vp}	$E_{mission}$
		G_1	G_2	G_3	G_6	G_8	G_9	G_{12}		
MONTSA	MF_{VP}	152.68	87.37	61.68	100	397.81	100	364.34	**42697.43**	1.6353
	ME	329.85	100	140	100	265.62	100	237.08	50334.45	**1.0363**
MOTSA	MF_{VP}	152.82	90.99	54.78	100	404.36	99.93	363.34	42896.19	1.6704
	ME	333.66	100	140	99.99	254.26	99.97	244.43	50337.39	1.0366
MOPSO	MF_{VP}	154.78	100	47.45	100	396.75	100	366.29	42985.48	1.6388
	ME	333.54	100	140	100	262.88	100	237.20	50521.81	1.0382

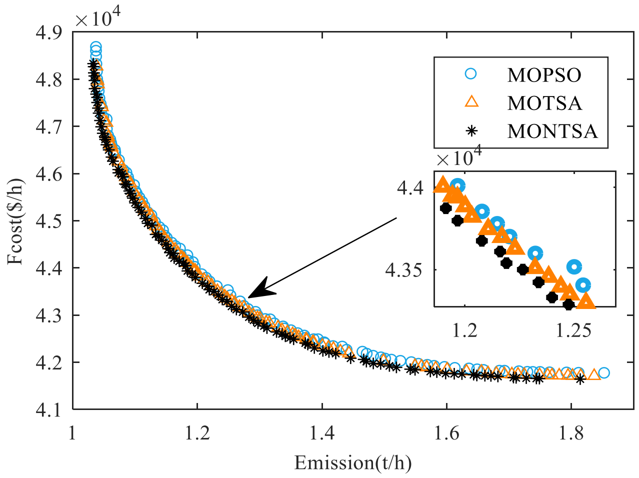

Fig. 11. The PFs obtained by several algorithms in Case 4

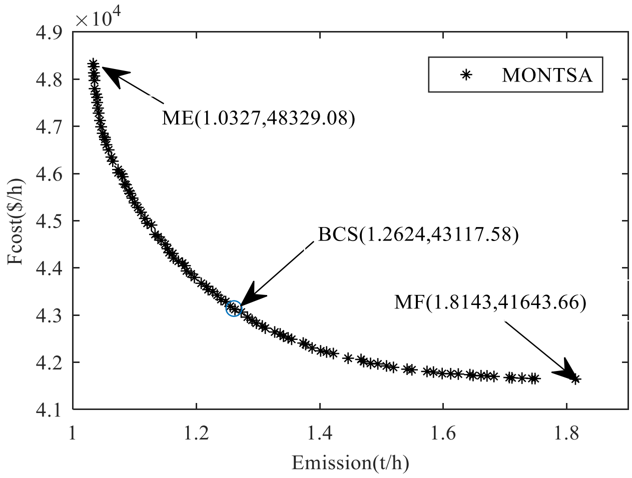

Fig. 12. The PF from MONTSA in Case 4

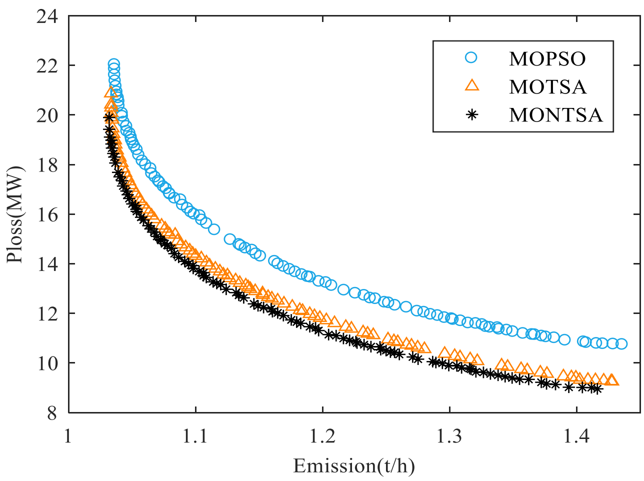

Fig. 13. The PFs obtained by several algorithms in Case 5

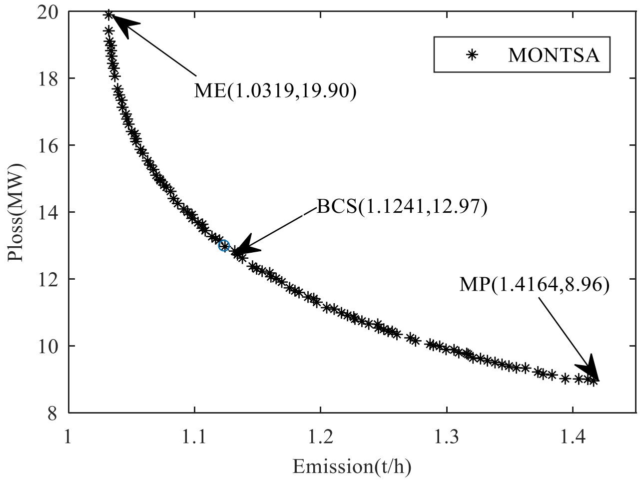

Fig. 14. The PF from MONTSA in Case 5

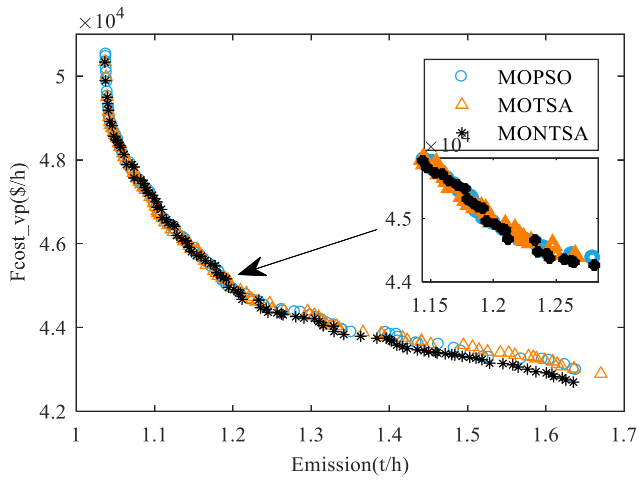

Fig. 15. The PFs obtained by several algorithms in Case 6

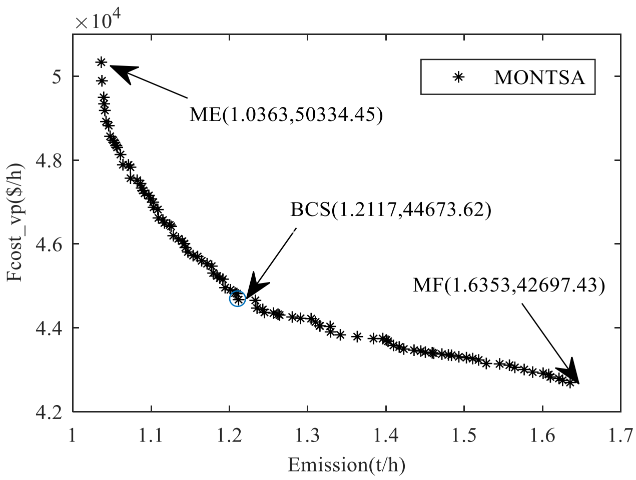

Fig. 16. The PF from MONTSA in Case 6

TABLE XIII
THE BCS AND CORRESPONDING POWER FOR CASE 5

Generators	MONTSA	MOTSA	MOPSO
G_1(MW)	227.19	226.88	221.23
G_2(MW)	99.82	100	100
G_3(MW)	139.96	139.14	140
G_6(MW)	99.99	99.73	100
G_8(MW)	274.73	276.97	280.86
G_9(MW)	99.98	99.98	100
G_{12}(MW)	322.1	321.52	323.42
P_{loss}(MW)	**12.97**	13.42	14.71
$E_{mission}$ (t/h)	**1.1241**	1.1266	1.1361

TABLE XIV
THE BCS AND CORRESPONDING POWER FOR CASE 6

Generators	MONTSA	MOTSA	MOPSO
G_1(MW)	228.86	229.83	229.50
G_2(MW)	99.55	99.52	100
G_3(MW)	104.21	109.15	110.73
G_6(MW)	100	100	100
G_8(MW)	341.13	300.10	298.20
G_9(MW)	100	99.90	100
G_{12}(MW)	292.15	328.02	327.57
F_{cost_vp}($/h)	**44673.62**	44950.04	45007.49
$E_{mission}$ (t/h)	**1.2117**	**1.1992**	**1.1925**

D. IEEE 118 test system

1) Case 7: Optimization experiment about F_{cost} and $E_{mission}$

The IEEE 118 bus system is a complex large system. To test the practicability of MONTSA in a large-scale system, bi-objectives F_{cost} and $E_{mission}$ are optimized simultaneously. Owing to the fact that MOPSO algorithm cannot acquire distributed convergent PF after 500 iterations, the classic MODE algorithm is selected as comparison algorithm. Fig. 17 leaves complete PFs of MONTSA, MOTSA and MODE algorithms, where the convergence and uniformity from integrated PF obviously are better than MOTSA and MODE algorithms. Fig. 18 enumerates the lower emission, fuel cost and BCS obtained by MONTSA.

TABLE XV reveals the lower emission and fuel cost obtained by three algorithms, where the lower emission and fuel cost obtained by MONTSA are 0.4678 (t/h) and 58659.7 ($/h), respectively. TABLE XVI indicates BCS obtained by three algorithms as well as corresponding generator units active power output. The BCS of MONTSA is 1.2773 (t/h) and 62426.35 ($/h), which is significantly better than results from other algorithms. It evinces that the proposed algorithm has better applicability in complex power systems.

2) Case 8: Optimization experiment about P_{loss} and $E_{mission}$

In the complex test system, P_{loss} and $E_{mission}$ are considered as optimization objectives in order to further research the association of economic and emission dispatch. The PFs of MONTSA, MOTSA and MODE algorithms are given in Fig. 19 and the PF obtained by MONTSA clearly dominates over comparison algorithms. The BCS and the boundary extreme obtained by MONTSA are presented in Fig. 20.

TABLE XVII shows the BCS and corresponding generator unit active power outputs obtained by the three algorithms. The BCS of MONTSA are 83.86 (MW) and 0.8005 (t/h), which account for the superiority over search results from comparison algorithms. TABLE XVIII indicates the boundary extreme obtained by optimization search process originated from three algorithms and the results obtained by MONTSA are 55.28 (MW) and 0.3995 (t/h). However, P_{loss} obtained by MODE algorithm is 48.25 (MW) and the reason is that the robustness about classical algorithm is excellent. By comparing the boundary extremes, PFs and BCS of other algorithms, it is found that the overall result of proposed algorithm is still better than the comparison algorithms. The above results demonstrate the effectiveness and practicality of enhanced algorithm in complex systems.

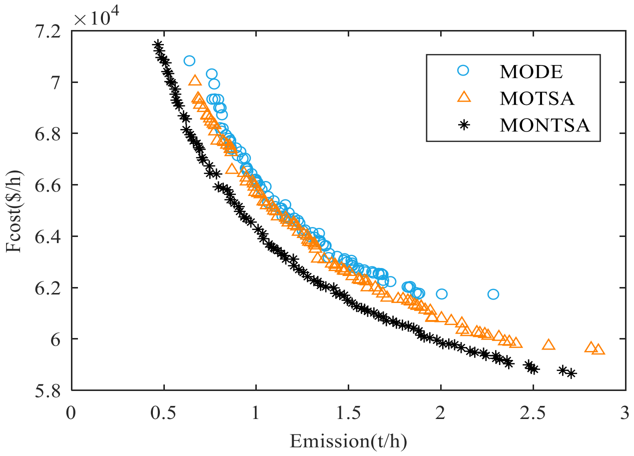

Fig. 17. The PFs obtained by several algorithms in Case 7

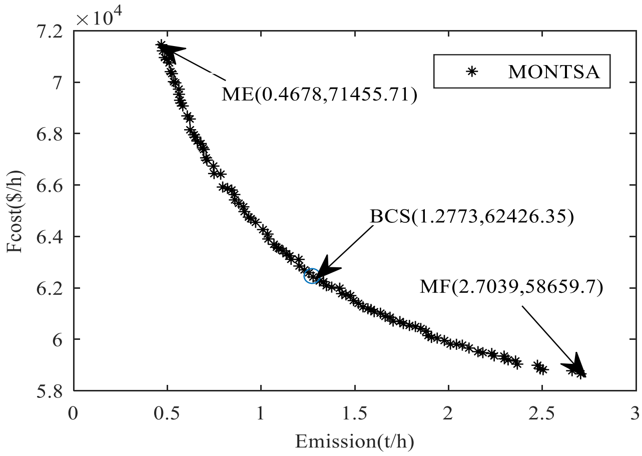

Fig. 18. The PF from MONTSA in Case 7

TABLE XV
THE CONCRETE RESULTS ABOUT *MP* AND *ME* FOR CASE 7

Algorithm	Object	F_{cost}	$E_{mission}$
MONTSA	*MF*	**58659.70**	2.7039
	ME	71455.71	**0.4678**
MOTSA	*MF*	59544.86	2.8511
	ME	70016.64	0.6685
MODE	*MF*	61702.98	2.2880
	ME	70791.13	0.6437

TABLE XVI
THE BCS AND CORRESPONDING POWER FOR CASE 7

Generators	MONTSA	MOTSA	MODE	Generators	MONTSA	MOTSA	MODE
G_{4}(MW)	10.83	5.30	5	G_{66}(MW)	122.28	114.20	100
G_{6}(MW)	6.41	9.47	8.05	G_{69}(MW)	-203.05	-201.68	-148.41
G_{8}(MW)	5.61	6.65	7.55	G_{70}(MW)	30.51	30.54	32.55
G_{10}(MW)	283.90	298.53	276.59	G_{72}(MW)	10.15	10	11.12
G_{12}(MW)	298.48	280.65	292.67	G_{73}(MW)	6.86	5.37	9.34
G_{15}(MW)	11.09	12.61	23.97	G_{74}(MW)	5.13	5.00	5
G_{18}(MW)	86.47	86.93	100	G_{76}(MW)	25.30	25.80	25
G_{19}(MW)	5.14	5.18	5.89	G_{77}(MW)	25.93	29.81	31.42
G_{24}(MW)	5.11	6.29	10.76	G_{80}(MW)	293.09	300	256.52
G_{25}(MW)	100.17	100	100	G_{82}(MW)	33.29	26.49	54.12
G_{26}(MW)	100	111.78	101.13	G_{85}(MW)	11.17	10.99	11.27
G_{27}(MW)	9.19	9.27	8.53	G_{87}(MW)	241.04	228.78	184.24
G_{31}(MW)	8.68	8.29	21.57	G_{89}(MW)	138.39	187.27	176.31
G_{32}(MW)	100	62.25	100	G_{90}(MW)	8.01	8.56	9.04
G_{34}(MW)	8.13	8	8	G_{91}(MW)	23.66	20	20.84
G_{36}(MW)	25.70	25	25	G_{92}(MW)	153.54	197.79	193.20
G_{40}(MW)	8.07	9.54	8.93	G_{99}(MW)	203.04	197.04	191.09
G_{42}(MW)	8.08	8	8	G_{100}(MW)	223.99	207.11	118.07
G_{46}(MW)	25	73.77	100	G_{103}(MW)	8.04	8.35	8.78
G_{49}(MW)	248.96	244.49	243.99	G_{104}(MW)	25.70	45.29	30.07
G_{54}(MW)	50.45	50	50	G_{105}(MW)	42.07	72.51	48.65
G_{55}(MW)	25	25	28.05	G_{107}(MW)	8.32	11.20	8
G_{56}(MW)	25.02	31.08	26.07	G_{110}(MW)	26.45	27.44	31.60
G_{59}(MW)	50.02	51.58	50.87	G_{111}(MW)	25	30.65	37.72
G_{61}(MW)	200	195.98	200	G_{112}(MW)	25	25	25
G_{62}(MW)	86.69	35.73	70.40	G_{113}(MW)	99.34	97.86	80.28
G_{65}(MW)	418.90	391.73	418.88	G_{116}(MW)	37.62	27.79	25
F_{cost} ($/h)	**62426.35**	63123.38	63133.91	**$E_{mission}$(t/h)**	**1.2773**	1.3322	1.3962

TABLE XVII
THE BCS AND CORRESPONDING POWER FOR CASE 8

Generators	MONTSA	MOTSA	MODE	Generators	MONTSA	MOTSA	MODE
G_{4}(MW)	25.80	30	30	G_{66}(MW)	100.00	100	100
G_{6}(MW)	28.67	30	25.62	G_{69}(MW)	-535.15	-201.68	-564.44
G_{8}(MW)	29.43	30	21.81	G_{70}(MW)	51.30	30	31.37
G_{10}(MW)	299.49	291.49	298.38	G_{72}(MW)	10.75	16.13	10.26
G_{12}(MW)	300	293.67	300	G_{73}(MW)	30	5	30
G_{15}(MW)	28.35	30	29.61	G_{74}(MW)	20	20	12.47
G_{18}(MW)	100	99.25	97.39	G_{76}(MW)	95.22	99.18	100
G_{19}(MW)	5	5	5.54	G_{77}(MW)	25.29	25.01	27.52
G_{24}(MW)	5	5	5	G_{80}(MW)	299.95	300	299.17
G_{25}(MW)	100	100.04	100.26	G_{82}(MW)	96.59	98.71	95.95
G_{26}(MW)	100.00	100	100.09	G_{85}(MW)	24.29	29.98	19.62
G_{27}(MW)	29.37	28.62	27.22	G_{87}(MW)	101.08	100.05	101.90
G_{31}(MW)	29.93	30	29.95	G_{89}(MW)	102.45	199.81	81.98
G_{32}(MW)	99.87	99.58	97.87	G_{90}(MW)	8.07	12.01	8.92
G_{34}(MW)	8.52	8.14	9.22	G_{91}(MW)	22.18	20.00	20
G_{36}(MW)	25	25	25.71	G_{92}(MW)	182.23	127.10	215.07
G_{40}(MW)	8.24	8.82	9.90	G_{99}(MW)	100	219.06	127.97
G_{42}(MW)	8.50	8	14.54	G_{100}(MW)	215.50	116.59	262.51
G_{46}(MW)	99.84	100	100	G_{103}(MW)	10.51	8.00	8
G_{49}(MW)	249.97	249.95	248.36	G_{104}(MW)	100	98.47	73.21
G_{54}(MW)	52.00	51.13	50.64	G_{105}(MW)	30.39	56.87	56.76
G_{55}(MW)	29.20	25.22	25	G_{107}(MW)	15.06	20	14.34
G_{56}(MW)	30.53	25.34	25	G_{110}(MW)	39.38	25.58	40.69
G_{59}(MW)	50.35	50	50	G_{111}(MW)	33.79	25.03	26.07
G_{61}(MW)	199.93	199.60	199.94	G_{112}(MW)	27.09	30.09	40.50
G_{62}(MW)	99.24	99.55	99.21	G_{113}(MW)	100	100.00	97.80
G_{65}(MW)	418.71	413.66	419.68	G_{116}(MW)	50.00	50	49.50
P_{loss}(MW)	**83.86**	100.11	100.01	**$E_{mission}$(t/h)**	**0.8005**	**0.7072**	**0.7022**

TABLE XVIII
THE CONCRETE RESULTS ABOUT *MP* AND *ME* FOR CASE 8

Algorithm	Object	P_{loss}	$E_{mission}$
MONTSA	*MP*	**55.28**	1.3795
	ME	149.29	**0.3995**
MOTSA	*MP*	62.93	1.5475
	ME	159.00	0.4375
MODE	*MP*	**48.25**	1.7223
	ME	183.56	0.4176

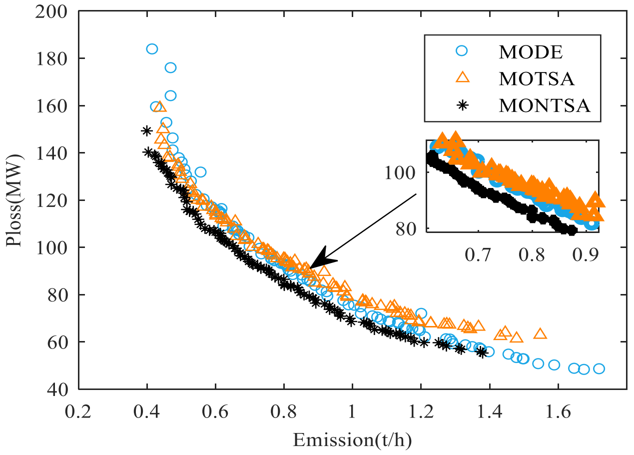

Fig. 19. The PFs obtained by several algorithms in Case 8

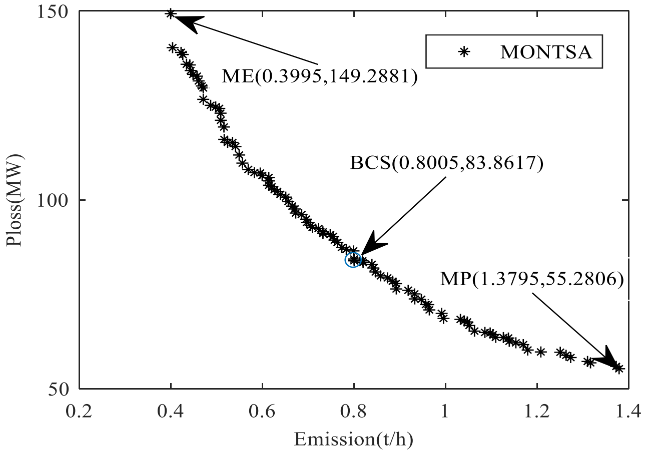

Fig. 20. The PF from MONTSA in Case 8

E. Performance evaluation

Performance metrics is primarily utilized to evaluate the merit of experimental results. To test the applicability about MONTSA comprehensively, *GD* and *HV* in the multi-objective evaluation system are selected as evaluation metrics. The *GD* index generally evaluates convergence of POS, while *HV* is a comprehensive index that principally evaluates convergence and diversity from POS, where diversity includes uniformity and extensiveness from the solution set.

1) GD

In the EED problem, the *GD* index is generally used to measure the convergence of PF, which chiefly represents minimum Euclidean distance between PF obtained by algorithm and real PF, and the definition is termed in the formula (21). The smaller *GD* value is, the better convergence from solution set is. When *GD* = 0, it indicates that real PF coincides with PF obtained by algorithm. In Case 1-8, *GD* index box plots from three algorithms are represented in Fig. 21.

$$GD = \frac{\sqrt{\sum_{i=1}^{n} d_i^2}}{n} \tag{21}$$

where n represents the number of solution sets; d_i indicates Euclidean distance between the ith solution and real PF.

2) HV

The *HV* index is frequently employed to evaluate convergence and diversity from PF, which mainly represents area volume in the objective space enclosed by the non-dominated solution set and the reference point obtained by algorithm. Essentially, it is to obtain volume covered by PF in the objective space domain and the definition is shown in the formula (22). The larger *HV* value is, the better diversity and convergence from the solution set are. Compared with *GD* index, there is no need to assume a reference set, which overcomes the deficiency of randomness. In Case 1-8, *HV* index box plots from three algorithms are shown in Fig. 22.

$$HV = volume\left(\bigcup_{i=1}^{N} v_i\right) \tag{22}$$

where v_i is volume formed by the ith solution and reference point.

3) Indicator result analysis

The average running time is considered as an evaluation about algorithm time complexity. TABLE XIX lists the average running times of several algorithms and it can be seen that the average running time of MONTSA is longer than original algorithm but shorter than classic algorithm.

Box plot is a common tool in the process of statistical data results, which can directly observe the mean, deviation and abnormal value. In Case 7-8, MOPSO algorithm does not converge. Therefore, MODE is regarded as replaced algorithm. Fig. 21 visually states minimum distance between real PF and PF obtained by three algorithms in all cases. Obviously, the results obtained by MONTSA in Case 1-6 are better than MOTSA and MOPSO as well as the results obtained by MONTSA in Case 7-8 dominate MOTSA and MODE. TABLE XX lists *GD* index mean and standard deviation about three algorithms. Compared with the rest of algorithms, MONTSA possesses a smaller mean and standard deviation. It undoubtedly indicates that PF obtained by MONTSA has good convergence and it has good applicability to deal with relevant cases.

Fig. 22 gives volume covered by PF in the objective space domain from three algorithms in all cases. Obviously, the diversity and convergence from the solution set obtained by MONTSA in Case 1-6 are better than MOTSA and MOPSO as well as the universality and uniformity from the solution set obtained by MONTSA in Case 7-8 significantly surpass MOTSA and MODE. TABLE XXI lists *HV* index mean and standard deviation of three algorithms. The mean and standard deviation of integrated algorithm are both greater than MOTSA and MOPSO/MODE. It reveals that PF obtained by MONTSA has good extensiveness and convergence and it has apparent advantages in EED problem.

TABLE XIX
THE AVERAGE RUNNING TIME FOR SEVERAL ALGORITHMS

Algorithm	Case							
	Case 1	Case 2	Case 3	Case 4	Case 5	Case 6	Case 7	Case 8
MONTSA	211.03	206.85	209.80	322.08	317.59	325.99	1600.10	1579.58
MOTSA	203.94	203.97	207.97	315.25	313.85	322.83	1535.83	1568.47
MOPSO	244.14	239.06	212.49	310.95	330.88	320.53	-	-
MODE	-	-	-	-	-	-	1556.71	1581.62

TABLE XX
THE MEAN AND STANDARD DEVIATION OF *GD* FOR SEVERAL ALGORITHMS

Index	Case	Statistics	Algorithm			
			MONTSA	MOTSA	MOPSO	MODE
GD	Case 1	mean	0.03144	0.03618	0.09505	-
		deviation	0.00912	0.01049	0.14745	-
	Case 2	mean	0.03260	0.03426	0.03882-	-
		deviation	0.00806	0.00884	0.01776	-
	Case 3	mean	0.00608	0.00982	0.01378	-
		deviation	0.00159	0.00307	0.00918	-
	Case 4	mean	0.45967	0.46037	1.01258	-
		deviation	0.12094	0.12198	0.37324	-
	Case 5	mean	0.03279	0.03939	0.09853	-
		deviation	0.01505	0.01856	0.04923	-
	Case 6	mean	0.43999	0.49151	0.55036	-
		deviation	0.12004	0.13807	0.15740	-
	Case 7	mean	0.60641	0.83744	-	1.12023
		deviation	0.15513	0.25236	-	0.38287
	Case 8	mean	0.07193	0.10902	-	0.11232
		deviation	0.02623	0.03582	-	0.04682

TABLE XXI
THE MEAN AND STANDARD DEVIATION OF *HV* FOR SEVERAL ALGORITHMS

Index	Case	Statistics	Algorithm			
			MONTSA	MOTSA	MOPSO	MODE
HV	Case 1	mean	1.51319	0.40596	0.38426	-
		deviation	0.59076	0.00433	0.01084	-
	Case 2	mean	0.85115	0.44871	0.37723	-
		deviation	0.05511	0.00692	0.00572	-
	Case 3	mean	0.07239	0.05986	0.03534	-
		deviation	0.01260	0.00204	0.00114	-
	Case 4	mean	6062.38	4972.19	4935.52	-
		deviation	566.290	191.456	125.211	-
	Case 5	mean	7.59773	6.39505	5.87920	-
		deviation	0.74649	0.51391	0.44988	-
	Case 6	mean	7646.15	6707.54	6635.67	-
		deviation	814.506	630.132	656.918	-
	Case 7	mean	39662.09	39593.87	-	12126.22
		deviation	1385.53	1524.64	-	1369.65
	Case 8	mean	361.505	184.990	-	134.386
		deviation	39.3179	21.8605	-	12.3374

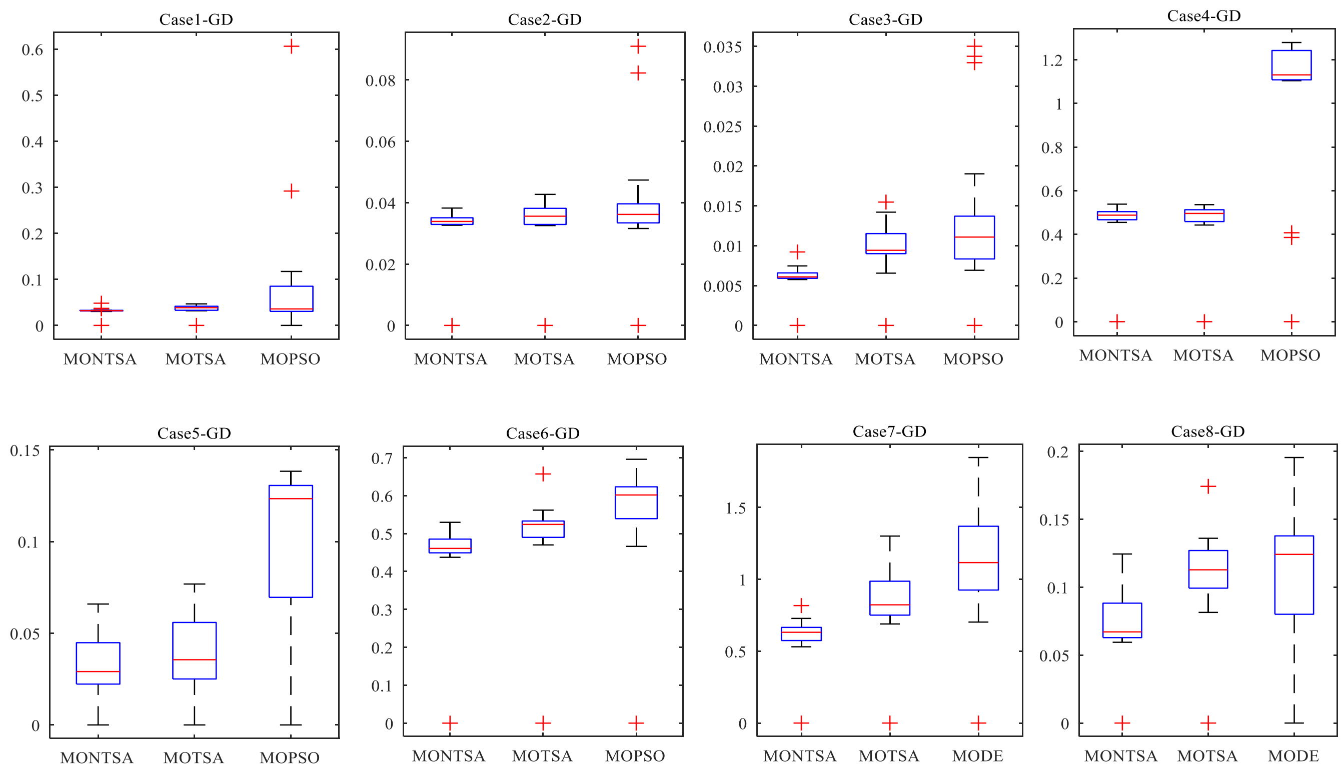

Fig. 21. Boxplots of *GD* for several algorithms

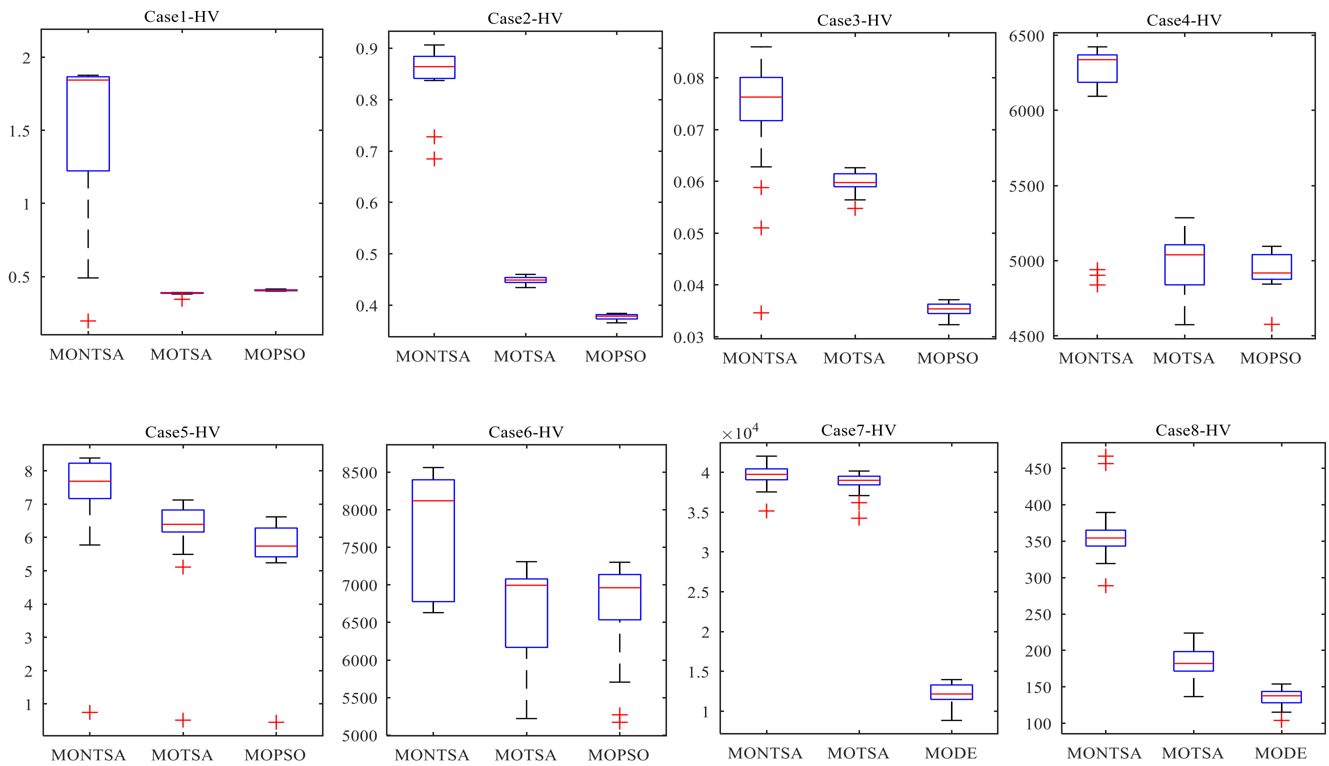

Fig. 22. Boxplots of *HV* for several algorithms

V. CONCLUSION

For making sure stable, economical, and environmental operation from power system, for high dimensional, non-convex and nonlinear characteristics about EED problem, this article proposes a novel search algorithm-MONTSA, which contains DE variation process based on Cauchy mutation strategy, Gaussian distribution mutation mechanism as well as non-linear adaptive search tendency. MONTSA switches search equations to balance algorithms exploration and exploitation through *ST* and puts forward a novel constraint-dominant strategy handling techniques based on dynamic crowding distance to obtain a collection of better POS. In order to verify the effectiveness about enhanced algorithm, three algorithms are applied to IEEE 30 bus, IEEE 57 bus and IEEE 118 bus test systems, containing eight cases. The obtained results turn out that PF and BCS obtained by MONTSA are superior to MOTSA and MOPSO/MODE. In addition, the result analysis of statistical indicators *GD* and *HV* reveals that convergence and diversity about POS acquired by MONTSA are significantly better than MOTSA and MOPSO/MODE. Therefore, the integrated algorithm employed to deal with EED problem has a certain reference significance.

REFERENCES

[1] G. Chen, X. Man, Y. Long, and Z. Zhang, "Application of multi-objective new whale optimization algorithm for environment economic power dispatch problem," *Engineering Letters*, vol. 29, no. 1, pp. 68-81, 2021.

[2] G. Chen, J. Qian, Z. Zhang, and Z. Sun, "Many-objective new bat algorithm and constraint-priority non-inferior sorting strategy for optimal power flow," *Engineering Letters*, vol. 27, no. 4, pp. 882-892, 2019.

[3] X. Zhao, J. Liang, J. Meng and Y. Zhou, "An improved quantum particle swarm optimization algorithm for environmental economic dispatch," *Expert Systems with Applications*, vol. 152, pp. 113-370, 2020.

[4] D. Das, A. Bhattacharya and R. N. Ray, "Dragonfly algorithm for solving probabilistic economic load dispatch problems," *Neural Computing & Applications*, vol. 32, no. 8, pp. 3029-3045, 2020.

[5] M. F. Tabassum, M. Saeed, N. A. Chaudhry, J. Ali, M. Farman and S. Akram, "Evolutionary simplex adaptive Hooke-Jeeves algorithm for economic load dispatch problem considering valve point loading effects," *Ain Shams Engineering Journal*, vol. 12, no. 1, pp. 1001-1015, 2021.

[6] M. Javadi, T. Amraee and F. Capitanescu, "Look ahead dynamic security-constrained economic dispatch considering frequency stability and smart loads," *International Journal of Electrical Power & Energy Systems*, vol. 108, pp. 240-251, 2019.

[7] F. X. Rugema, G. Yan, S. Mugemanyi, Q. Jia, S. Zhang and C. Bananeza, "A Cauchy-Gaussian quantum-behaved bat algorithm applied to solve the economic load dispatch problem," *IEEE Access*, vol. 9, pp. 3207-3228, 2021.

[8] M. A. Abido, "A novel multiobjective evolutionary algorithm or environmental/economic power dispatch," *Electric Power Systems Research*, vol. 65, no. 1, pp. 71-81, 2003.

[9] P. K. Hota, A. K. Barisal and R. Chakrabarti, "Economic emission load dispatch through fuzzy based bacterial foraging algorithm," *International Journal of Electrical Power & Energy Systems*, vol. 32, no. 7, pp. 794-803, 2010.

[10] L. Li, Z. Liu, M. Tseng, S. Zheng and M. K. Lim, "Improved tunicate swarm algorithm: Solving the dynamic economic emission dispatch problems," *Applied Soft Computing*, vol. 108, no. 5, pp. 107-504, 2021.

[11] V. P. Sakthivel, M. Suman and P. D. Sathya, "Combined economic and emission power dispatch problems through multi-objective squirrel search algorithm," *Applied Soft Computing*, vol. 100, pp. 106-950, 2021.

[12] J. Wang, X. He, J. Huang and G. Chen, "Recurrent neural network for non-convex economic emission dispatch," *Journal of Modern Power Systems and Clean Energy*, vol. 9, no. 1, pp. 46-55, 2021.

[13] B. Y. Qu, Y. S. Zhu, Y. C. Jiao, M. Y. Wu, P. N. Suganthan and J. J. Liang, "A survey on multi-objective evolutionary algorithms for the solution of the environmental/economic dispatch problems," *Swarm & Evolutionary Computation*, vol. 38, pp. 1-11, 2018.

[14] X. Li, X. Li, K. Wang, S. Yang and Y. Li, "Achievement scalarizing function sorting for strength Pareto evolutionary algorithm in many-objective optimization," *Neural Computing & Applications*, vol. 33, no. 11, pp. 6369-6388, 2021.

[15] G. Xiong, J. Zhang, D. Shi, L. Zhu, X. Yuan and Z. Tan, "Winner-leading competitive swarm optimizer with dynamic Gaussian mutation for parameter extraction of solar photovoltaic models," *Energy Conversion & Management*, vol. 206, pp. 112-450. 2020.

[16] R. Azizipanah-Abarghooee, P. Dehghanian and V. Terzija, "Practical multi-area bi-objective environmental economic dispatch equipped with a hybrid gradient search method and improved Jaya algorithm," *IET Generation Transmission & Distribution*, vol. 10, no. 14, pp. 3580-3596, 2016.

[17] G. Chen, X. Yi, Z. Zhang and H. Wang, "Applications of multi-objective dimension-based firefly algorithm to optimize the power losses, emission, and cost in power systems," *Applied Soft Computing*, vol. 68, pp. 322-342, 2018.

[18] A. A. Abou El Ela, M. A. Abido and S. R. Spea, "Differential evolution algorithm for emission constrained economic power dispatch problem," *Electric Power Systems Research*, vol. 80, no. 10, pp. 1286-1292, 2010.

[19] M. A. Abido, "Multiobjective particle swarm optimization for environmental/economic dispatch problem," *Electric Power Systems Research*, vol. 79, no. 7, pp. 1105-1113, 2009.

[20] V. Savsani and M. A. Tawhid, "Non-dominated sorting moth flame optimization (NS-MFO) for multi-objective problems," *Engineering Applications of Artificial Intelligence*, vol. 63, pp. 20-32, 2017.

[21] X. Yuan, B. Zhang, P. Wang, J. Liang, Y. Yuan and Y. Huang, "Multi-objective optimal power flow based on improved strength Pareto evolutionary algorithm," *Energy*, vol. 122, pp. 70-82, 2017.

[22] M. S. Kiran, "TSA: Tree-seed algorithm for continuous optimization," *Expert Systems with Applications*, vol. 42, no. 19, pp. 6686-6698, 2015.

[23] A. A. El-Fergany and H. M. Hasanien, "Tree-seed algorithm for solving optimal power flow problem in large-scale power systems incorporating validations and comparisons," *Applied Soft Computing*, vol. 64, pp. 307-316, 2018.

[24] I. Gungor, B. G. Emiroglu, A. C. Cinar and M. S. Kiran, "Integration search strategies in tree seed algorithm for high dimensional function optimization," *International Journal of Machine Learning & Cybernetics*, vol. 11, no. 2, pp. 249-267, 2020.

[25] J. Jiang, M. Xu, X. Meng and K. Li, "STSA: A sine Tree-Seed Algorithm for complex continuous optimization problems," *Physica A: Statistical Mechanics & its Applications*, vol. 537, pp., 2020.

[26] A. C. Cinar, "Training feed-forward multi-layer perceptron artificial neural networks with a Tree-Seed Algorithm," *Arabian Journal for Science & Engineering*, vol. 45, no. 12, pp. 10915-10938, 2020.

[27] A. Babalik, A. C. Cinar and M. S. Kiran, "A modification of tree-seed algorithm using Deb's rules for constrained optimization," *Applied Soft Computing*, vol. 63, pp. 289-305, 2018.

[28] S. Barshandeh and M. Haghzadeh, "A new hybrid chaotic atom search optimization based on tree-seed algorithm and Levy flight for solving optimization problems," *Engineering with Computers*, pp. 1-44, 2020.

[29] L. While, L. Bradstreet and L. Barone, "A fast way of calculating exact hypervolumes," *IEEE Transactions On Evolutionary Computation*, vol. 16, no. 1, pp. 86-95, 2012.

[30] H. Ishibuchi, R. Imada, Y. Setoguchi and Y. Nojima, "Reference point specification in inverted generational distance for triangular linear pareto front," *IEEE Transactions on Evolutionary Computation*, vol. 22, no. 6, pp. 961-975, 2018.

[31] G. Chen, J. Qian, Z. Zhang and Z. Sun, "Multi-objective optimal power flow based on hybrid firefly-bat algorithm and constraints-prior object-fuzzy sorting strategy," *IEEE Access*, vol. 7, pp. 139726-139745, 2019.

[32] W. Gao, F. T. S. Chan, L. Huang and S. Liu, "Bare bones artificial bee colony algorithm with parameter adaptation and fitness-based neighborhood," *Information Sciences*, vol. 316, pp. 180-200, 2015.

[33] S. Wang, Y. Li and H. Yang, "Self-adaptive differential evolution algorithm with improved mutation mode," *Applied Intelligence*, vol. 47, no. 3, pp. 644-658, 2017.

[34] R. Salgotra and U. Singh, "Application of mutation operators to flower pollination algorithm," *Expert Systems with Applications*, vol. 79, pp. 112-129, 2017.

[35] K. Deb, A. Pratap, S. Agarwal and T. Meyarivan, "A fast and elitist multiobjective genetic algorithm: NSGA-II," *IEEE Transactions on Evolutionary Computation*, vol. 6, no. 2, pp. 182-197, 2002.

[36] A. Ghasemi, "A fuzzified multi objective interactive honey bee mating optimization for environmental/economic power dispatch with valve point effect," *International Journal of Electrical Power & Energy Systems*, vol. 49, pp. 308-321, 2013.

[37] G. Chen, J. Qian, Z. Zhang and Z. Sun, "Applications of novel hybrid bat algorithm with constrained pareto fuzzy dominant rule on multi-objective optimal power flow problems," *IEEE Access*, vol. 7, pp. 52060-52084, 2019.

[38] R.T.F.A. King, H.C.S. Rughooputh, and K. Deb, "Solving the multi-objective environmental/economic dispatch problem with prohibited operating zones using NSGA-II," *IEEE*, vol. 41, pp. 298-303, 2011.

[39] B.K. Panigrahi, V.R. Pandi, S. Das, and S. Das, "Multiobjective fuzzy dominance based bacterial foraging algorithm to solve economic emission dispatch problem," *Electric Power Systems Research*, vol. 25, pp. 97-105, 2003.

[40] S. Hemamalini and S.P. Simon, "Emission constrained economic dispatch with valve-point effect using particle swarm optimization," *IEEE Xplore*, vol. 1, pp. 1-6, 2008.

[41] T. Liu, L. Jiao, W. Ma, J. Ma, and R. Shang, "Cultural quantum-behaved particle swarm optimization for environmental/economic dispatch," *Applied Soft Computing*, vol. 48, pp. 597-611, 2016.